

Vacancy structure in Prussian blue analogues

Max Krummenacher

Semester project HS23
BSc material science and engineering ETH Zürich
supervised by Arkadiy Simonov

Abstract

Prussian blue analogues is family of inorganic compounds. Due to their complex microporous structure they have found applications in gas storage, battery application and metal ion immobilization. Using a Monte Carlo simulation their structure was modeled in silico. Additionally, the infrastructure to work with .mmcif, the calculation of structure factors and support for the Yell format was developed in Python. Using diffuse scattering and simulated energies it was successfully shown that phase transitions take place in the simulation.

1. Introduction

1.1. Prussian Blue Analogues

For the purposes of this report we consider Prussian blue analogues (PBA) to be compounds with composition $M[M'(CN)_6]_x$ where M and M' are transition metals and x is the fill fraction of the hexacyanometalates. The idealized structure of these compounds is the face centered cubic structure shown in Figure 1 [1].

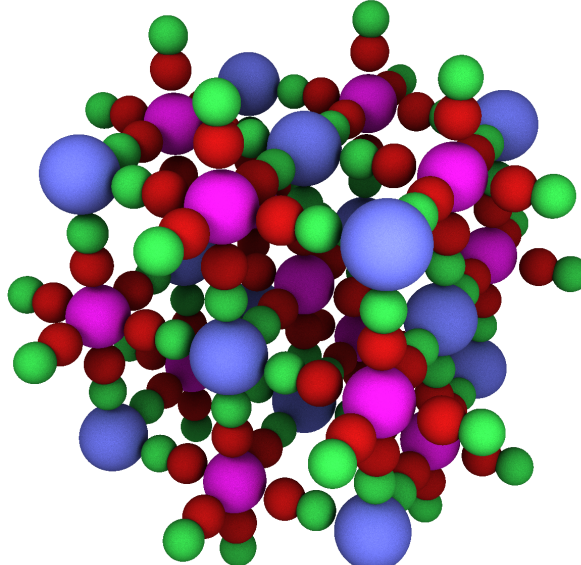


Figure 1: The structure of $M[M'(CN)_6]$

However this exact structure is only achievable if the M ion has the same charge as the $[M'(CN)_6]$ ion, in other words if charge balance allows $x = 1$. An example of such a PBA is $Mn[Pt(CN)_6]$. If this condition is not met then some of the hexacyanometalate sites remain unoccupied.

Prussian blue itself has the composition $Fe^{III}[Fe^{II}(CN)_6]_{\frac{3}{4}}$ [2]. The fill fraction of $\frac{3}{4}$ allows the vacancies to be arranged in a periodic fashion in the cubic crystal structure shown in Figure 2. These vacancies aren't true vacancies in the strict sense. They don't remain empty. In the case of Prussian

blue they are filled with water or depending on the production method might even be filled with alkali metal ions. [3] This further complicates the condition of charge balance and is one of the reasons why the structure of Prussian blue has long been a mystery.

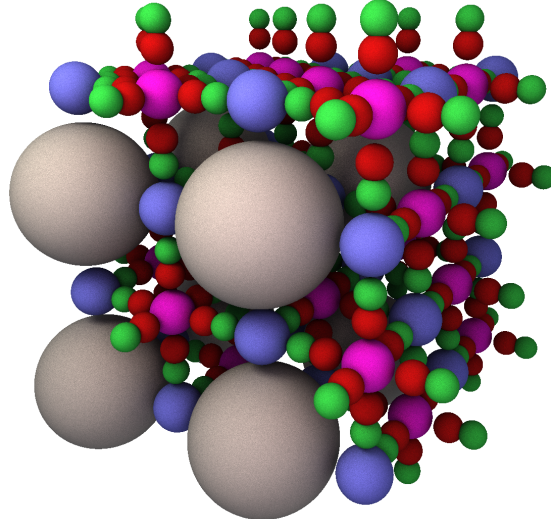


Figure 2: Arrangement of vacancies in Prussian blue

In other PBAs like for example $\text{Mn}^{\text{II}}[\text{Co}^{\text{III}}(\text{CN})_6]$, the fill fraction might not allow for a periodic arrangement of vacancies in a cubic crystal. This leads the crystal to be a frustrated system, as there is no singular state with lowest energy.

The collection of vacancies cause the crystal to have a microporous structure.[4] If two vacancies lie next to each other they connect to form a larger micropore. Thus the structure of vacancies in the crystal is important for many transport properties of the bulk material. Prussian blue has found application in medicine against Cs poisoning as Cs ions fit within the vacancies of the crystal where they remain immobilized[5]. Other applications for the microporosity of PBAs include the storage of gases (eg. Hydrogen)[6] and the use in batteries [4], [7].

In this paper we explore the arrangement of vacancies of PBA with fill fraction $x = \frac{1}{3}$ through a Monte Carlo simulation using a simple nearest and next nearest neighbor interaction approximation for the Hamiltonian.

1.2. Diffuse scattering

Diffraction is a common crystallographic method by which crystal structure and crystal parameters can be determined. In the diffraction experiments a beam of monochromatic X-rays is diffracted by a single crystal. This causes the beam to diffract at the atoms according to the following formula [8]:

$$F_{hkl} = \sum_j f_j \exp\left(2\pi i(h \ k \ l) \begin{pmatrix} x_j \\ y_j \\ z_j \end{pmatrix}\right) \quad (1)$$

Where F_{hkl} is the complex structure factor at position $(h \ k \ l)$ in the reciprocal space, f_j is the atomic form factor of the atom at position $\begin{pmatrix} x_j \\ y_j \\ z_j \end{pmatrix}$. In a perfect infinitely large crystal the structure factor is zero everywhere except at integer valued $(h \ k \ l)$. Note that the Laue method measures the intensity $I = |F|^2$ such that the phase of F_{hkl} is lost.

If the periodicity of the crystal is broken an additional diffuse signal appears. However if there is some statistical pattern in the aperiodicity of the crystal (as in PBAs) the change of the shape of the peaks is characteristic of this statistical pattern. [9]

1.3. Monte Carlo Simulation

For a system, of which we know all possible states $\sigma \in \Omega$ and the Hamiltonian for each state $\mathcal{H}(\sigma)$, we can obtain a macroscopic view of the system by the Monte Carlo method. Suppose the probability of a state occurring $\rho(\sigma)$ at some temperature $T > 0$ is proportional to $\exp\left(-\frac{\mathcal{H}(\sigma)}{k_b T}\right)$. [10] We know the probabilities sum to 1.

$$1 = \sum_{\sigma \in \Omega} \frac{\exp\left(-\frac{\mathcal{H}(\sigma)}{k_b T}\right)}{Z} = \frac{1}{Z} \sum_{\sigma \in \Omega} \exp\left(-\frac{\mathcal{H}(\sigma)}{k_b T}\right) \quad (2)$$

$$\Rightarrow Z = \sum_{\sigma \in \Omega} \exp\left(-\frac{\mathcal{H}(\sigma)}{k_b T}\right) \quad (3)$$

thus:

$$\rho(\sigma) = \frac{\exp\left(-\frac{\mathcal{H}(\sigma)}{k_b T}\right)}{Z} \quad (4)$$

We define macroscopic variables of state in terms of the expected value of their associated microscopic variables. [10] For example for the internal energy we define:

$$U = \langle \mathcal{H} \rangle = \sum_{\sigma \in \Omega} \mathcal{H}(\sigma) \rho(\sigma) \quad (5)$$

Although each term of these sums are simple set of states over which the sum is taken are often mathematically complex and as such very hard to solve analytically. Though these sums are computable for systems with a small number of states to obtain statistically relevant results a large system needs to be chosen and the calculation of the expectance value becomes computationally expensive. In the Monte Carlo simulation we find an approach to calculate the expected value of these variables without iterating through all states.

The fundamental idea behind the technique is to generate a series of states σ_i drawn from the probability distribution defined by $\rho(\sigma)$ (Equation 4). Variables of state can then be calculated as the average of the microscopic variable.

For this simulation these draws are generated by the following process:

- 1) Start with some randomly generated state.
- 2) Make a small change to the state.
- 3) Compare the Hamiltonians of the states.
 - a) If the Hamiltonian is lower in the new state the new state is accepted.
 - b) If the Hamiltonian is higher the new state is accepted with probability $p = \exp\left(-\frac{\Delta\mathcal{H}}{k_b T}\right)$.
- 4) back to step 2)

Also shown in Figure 3.

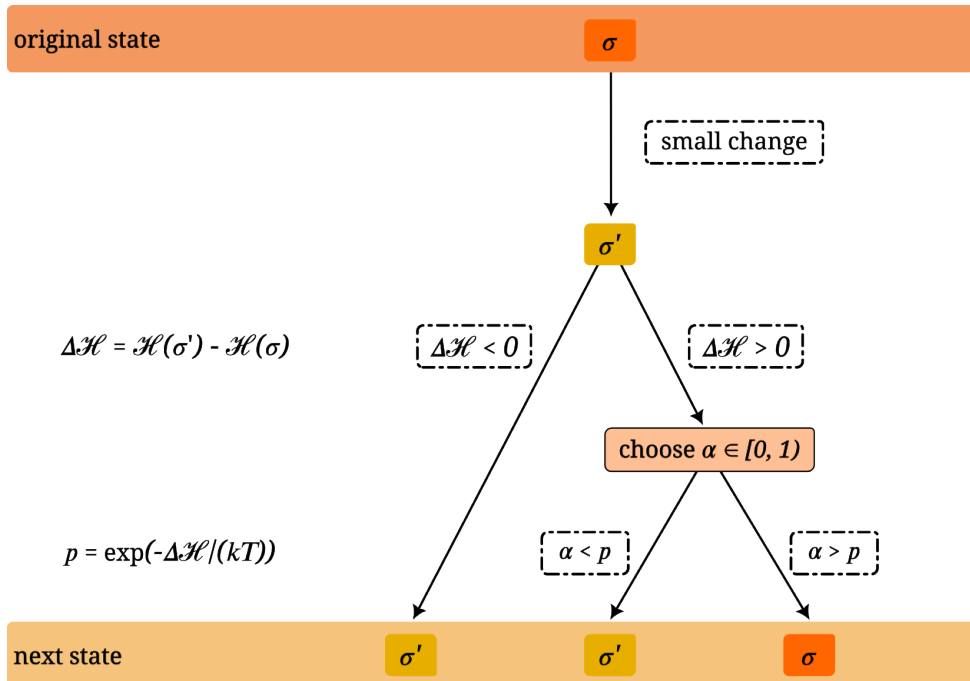


Figure 3: Diagram showing one Monte Carlo step

For this process to form the probability distribution $\rho(\sigma)$ whenever a new temperature is chosen, the system needs to equilibrate. In other words the system needs to reach a state somewhat typical for the temperature plugged in and from then on the states follow the probability distribution. To reach this state the Monte Carlo steps are repeated for a set number of steps.

At low temperatures T the probability of a change in state being accepted is very small. This leads the distribution of states to converge to wanted distribution very slowly. Slow convergence at low temperatures is one of the biggest shortcomings of the Monte Carlo method.

2. Methods

2.1. Simulation

The simulation program was written in Rust.

2.1.1. States

The structure is modeled as a three dimensional square grid containing N unit cells. To represent the fcc structure of the PBA, a grid of size $2N \times 2N \times 2N$ is created and all positions with $i + j + k \equiv 0 \pmod{2}$ are populated with 0 representing the fixed M sites. The other positions are populated with -1 or 1 representing a vacancy or a cyanometalate respectively. To achieve the exact fill fraction a vector containing the correct number of -1 and 1 is generated and then shuffled to achieve a random starting state. Note that this creates a three dimensional version of a checkerboard pattern where each direct neighbor to an -1/1 site is a 0 site. Additionally, the grid is accessed in a modular fashion such that $e_{i,j,k} = e_{i+2N,j,k} = e_{i,j+2N,k} = e_{i,j,k+2N}$.

2.1.2. Hamiltonian

The Hamiltonian of the system is divided into 2 terms. Only interactions between cyanometalates and vacancies are considered. For the nearest neighbor with an offset of $\frac{1}{2}\langle 110 \rangle$ if both of them are the same (vacancies or metalates) their contribution to the total energy is J_1 otherwise it is $-J_1$. Similarly for next nearest neighbors along $\langle 100 \rangle$ directions, if both are the same their contribution is J_2 , $-J_2$ otherwise.

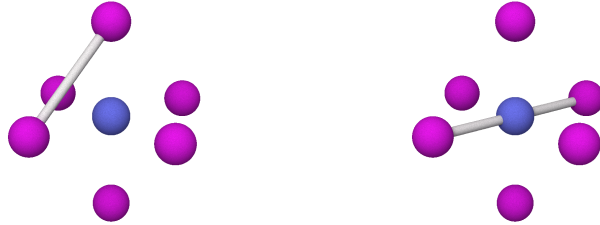


Figure 4: Images showing the nearest and next nearest neighbors of M' around M left, right respectively

Let $I = \{(i, j, k) \mid i + j + k \equiv 1 \pmod{2}, 0 \leq i, j, k < 2N\}$ be the set of all indexes of possible cyanometalate sites and $\sigma_{i,j,k}$ the value at index (i, j, k) . With this notation we can express the Hamiltonian in the following way:

$$\begin{aligned} \mathcal{H}(\sigma) &= \sum_{\vec{r}_0 \in I} \left(\frac{1}{2} \sum_{\vec{r} \in \langle 110 \rangle} J_1 \sigma_{\vec{r}_0} \sigma_{\vec{r}_0 + \vec{r}} + \frac{1}{2} \sum_{\vec{r} \in \langle 100 \rangle} J_2 \sigma_{\vec{r}_0} \sigma_{\vec{r}_0 + \vec{r}} \right) \\ &= J_1 \left(\frac{1}{2} \sum_{\vec{r}_0 \in I} \sum_{\vec{r} \in \langle 110 \rangle} \sigma_{\vec{r}_0} \sigma_{\vec{r}_0 + \vec{r}} \right) + J_2 \left(\frac{1}{2} \sum_{\vec{r}_0 \in I} \sum_{\vec{r} \in \langle 100 \rangle} \sigma_{\vec{r}_0} \sigma_{\vec{r}_0 + \vec{r}} \right) \\ &= J_1 s_1(\sigma) + J_2 s_2(\sigma) \end{aligned} \quad (6)$$

Where the factors of $\frac{1}{2}$ correct for counting each neighbor interaction twice and the functions $s_1(\sigma)$ and $s_2(\sigma)$ correspond to the sum over nearest neighbor and next nearest neighbor respectively. (Note that here $\langle 110 \rangle$ and $\langle 100 \rangle$ correspond to offsets of the indexes into the array and not crystallographic

vectors)

Instead of calculating the Hamiltonian directly the sums s_1 and s_2 are computed and updated in each step. As these sums are of integer value they allow faster computation and avoid float inaccuracies.

2.1.3. Parameters

For each Monte Carlo step two of the vacancy/cyanometalate sites, which aren't the same are chosen uniformly from the whole grid. To calculate the difference in energy, if a swap was to be performed is calculated by calculating how the sums over nearest neighbors and next nearest neighbors. If this difference in energy is smaller than zero the swap is accepted, otherwise the swap is accepted with a probability $p = \exp\left(-\frac{\Delta\mathcal{H}}{k_b T}\right)$.

As by the consideration in the appendix (Equation 8) only two new parameters $J' = \frac{J_1}{J_2}$ and $T' = \frac{k_b T}{J_2}$ need to be explored to get an overview over the whole parameter space. For the simulation an ensemble of 20 models with different J' terms is simulated. Each model is tempered from some initial temperature T_0 to T_{n-1} . The temperature steps are chosen such that $\ln(T_i)$ is a linear function of i . At each temperature the model is left to equilibrate for 500 epochs before any measurements are taken from another 500 epochs. Where an epoch refers to 8S Monte Carlo steps with the number of vacancy/cyanometalate sites S .

2.1.4. Output

At the end of each temperature step a .mmcif file is generated from the model, which is a crystallographic file format that contains information about positions of atoms in the supercell. All values from the measurements are logged to a .csv file.

2.1.5. Optimizations

For the compiler to be able to fully optimize the program, where possible the size of list of values, like the grid is given at compile time through the use of [i8; N] instead of Vec<i8>. Though the Monte Carlo method itself is not parallelizable many systems of different J' 's can be run at the same time. For this the crate rayon was used.

2.2. Data Analysis

On the .mmcif files produced by the simulation the command line tool gemmi sfcalc is run. This program calculates the structure factors using the fast Fourier transform for the crystal provided in the input file. gemmi is called from a python script which then converts the data into the Yell format.

3. Results

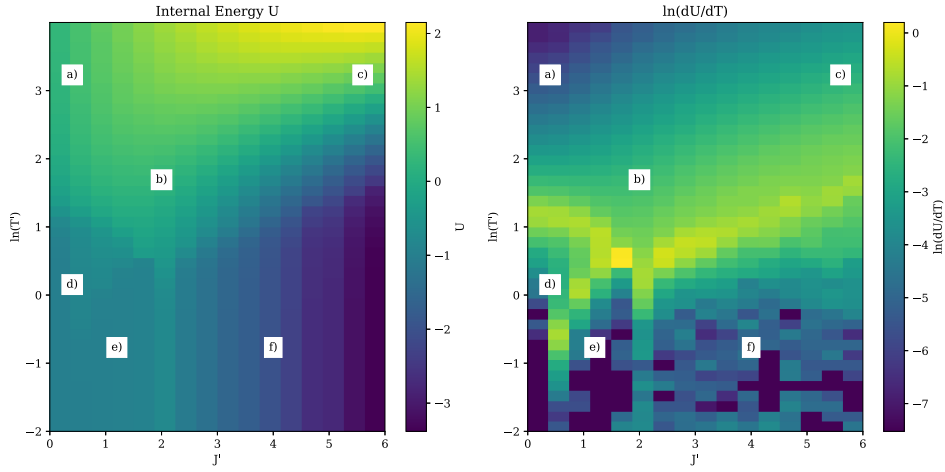


Figure 5: Internal Energy of the system and the natural log of its derivative with respect to temperature

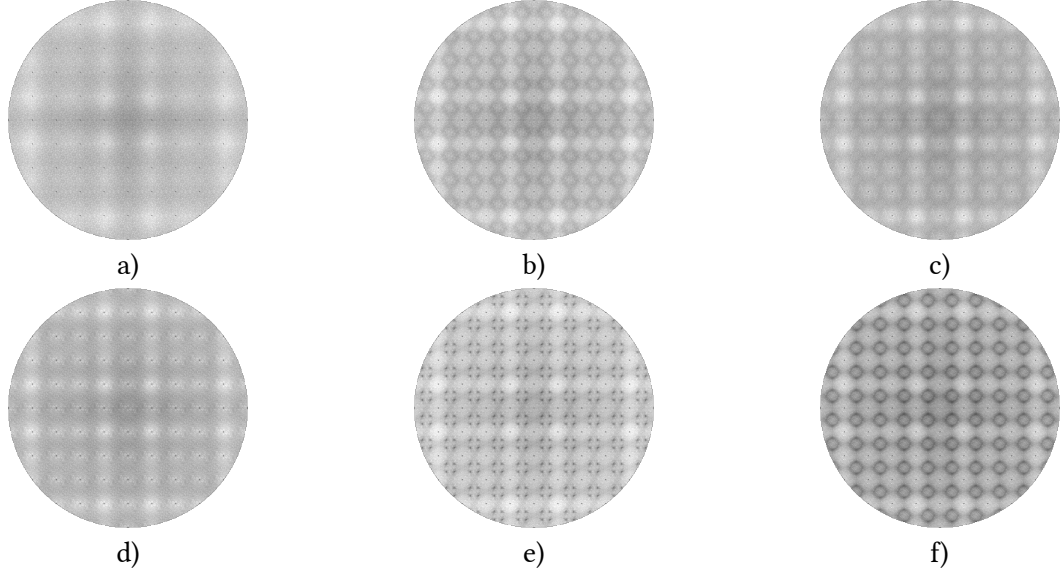


Figure 6: Diffraction patterns at the positions labeled in Figure 5

Figure 5 shows the energy calculated during the simulation. In the plot of the derivative of the internal energy invalid values resulting from the log were replaced by the minimum values. The diffraction patterns at the the positions labeled in Figure 5 are shown in Figure 6.

4. Discussion

In Figure 5 phase transitions can be clearly recognized. In the plot of the derivative of the internal energy with respect to temperature we can see the limitations of the Monte Carlo method at lower temperatures. This is to be expected as the at lower temperatures more ordered structures are expected. and the structure might be in a local minimum of energy which cannot be left because of the low thermal energy. The change of the structures can be seen in the diffraction pattern in Figure 6. As expected we see very diffuse scattering at higher temperatures, while the diffraction patterns become more ordered at lower temperatures.

The Python module written for this project makes it easy to work with large numbers of .mmcif files and allows their structure factors to be calculated.

Furthermore the simulation could be generalized to include more distant neighbor interactions to create a better approximation of the real crystals.

Bibliography

- [1] B. Singh and A. Indra, “Prussian blue- and Prussian blue analogue-derived materials: progress and prospects for electrochemical energy conversion”, *Materials Today Energy*, vol. 16, p. 100404, 2020, doi: <https://doi.org/10.1016/j.mtener.2020.100404>.
- [2] B. Chadwick and A. Sharpe, “Transition Metal Cyanides and Their Complexes”, vol. 8. in *Advances in Inorganic Chemistry and Radiochemistry*, vol. 8. Academic Press, pp. 83–176, 1966. [Online]. Available: <https://www.sciencedirect.com/science/article/pii/S0065279208602010>
- [3] J. F. KEGGIN and F. D. MILES, “Structures and Formulae of the Prussian Blues and Related Compounds”, *Nature*, vol. 137, no. 3466, pp. 577–578, Apr. 1936, doi: 10.1038/137577a0.
- [4] K. Hurlbutt, S. Wheeler, I. Capone, and M. Pasta, “Prussian Blue Analogs as Battery Materials”, *Joule*, vol. 2, no. 10, pp. 1950–1960, 2018, doi: <https://doi.org/10.1016/j.joule.2018.07.017>.
- [5] P. A. Haas, “A Review of Information on Ferrocyanide Solids for Removal of Cesium from Solutions”, *Separation Science and Technology*, vol. 28, no. 17–18, pp. 2479–2506, 1993.
- [6] S. S. Kaye and J. R. Long, “Hydrogen Storage in the Dehydrated Prussian Blue Analogues M₃[-Co(CN)₆]₂ (M = Mn, Fe, Co, Ni, Cu, Zn)”, *Journal of the American Chemical Society*, vol. 127, no. 18, pp. 6506–6507, 2005.
- [7] B. Wang *et al.*, “Prussian Blue Analogs for Rechargeable Batteries”, *iScience*, vol. 3, pp. 110–133, 2018, doi: <https://doi.org/10.1016/j.isci.2018.04.008>.
- [8] U. Shmueli, Ed., *International tables for crystallography*. Chester, England: International Union of Crystallography, 2006.
- [9] A. Simonov, “Hidden diversity of vacancy networks in Prussian blue analogues”, *Nature*, vol. 578.
- [10] R. Baxter, *Exactly solved models in statistical mechanics*. London, England: ACADEMIC PRESS LIMITED, 1989.

5. Appendix

5.1. Considerations about the parameter space

Lets consider the Boltzmann factor of a system where the Hamiltonian \mathcal{H} can be described by the sum of two energies multiplied by two functions s_1 and s_2 on the state of the system σ .

$$\mathcal{H}(\sigma) = J_1 s_1(\sigma) + J_2 s_2(\sigma) \quad (7)$$

Lets define two new variables J' and T' such that $J_2 J' = J_1$ and $J_2 T' = k_b T$.

$$\begin{aligned} \exp\left(-\frac{\mathcal{H}(\sigma)}{k_b T}\right) &= \exp\left(-\frac{J_1 s_1(\sigma) + J_2 s_2(\sigma)}{k_b T}\right) \\ &= \exp\left(-\frac{\cancel{J}_2 J' s_1(\sigma) + \cancel{J}_2 s_2(\sigma)}{\cancel{J}_2 T'}\right) \\ &= \exp\left(-\frac{J' s_1(\sigma) + s_2(\sigma)}{T'}\right) \end{aligned} \quad (8)$$

Thus we can describe the whole parameter space using only T' and J' .

5.2. Note on images

Figure 1, Figure 2 and Figure 4 are rendered using a ray tracer written in rust <https://github.com/max-kay/ray>.

5.3. Additional material

All code used for this project including the source for this report and presentation slides can be found on GitHub.

<https://github.com/max-kay/pba>